

# Journal of Materials Chemistry B

Accepted Manuscript



This is an *Accepted Manuscript*, which has been through the Royal Society of Chemistry peer review process and has been accepted for publication.

*Accepted Manuscripts* are published online shortly after acceptance, before technical editing, formatting and proof reading. Using this free service, authors can make their results available to the community, in citable form, before we publish the edited article. We will replace this *Accepted Manuscript* with the edited and formatted *Advance Article* as soon as it is available.

You can find more information about *Accepted Manuscripts* in the [Information for Authors](#).

Please note that technical editing may introduce minor changes to the text and/or graphics, which may alter content. The journal's standard [Terms & Conditions](#) and the [Ethical guidelines](#) still apply. In no event shall the Royal Society of Chemistry be held responsible for any errors or omissions in this *Accepted Manuscript* or any consequences arising from the use of any information it contains.

## Enzyme-catalyzed *in situ* forming gelatin hydrogels as bioactive wound dressings: Effect of fibroblast delivery on wound healing efficacy

Cite this: DOI: 10.1039/x0xx00000x

Yunki Lee,<sup>a</sup> Jin Woo Bae,<sup>a</sup> Jin Woo Lee,<sup>b</sup> Wonhee Suh,<sup>c</sup> and Ki Dong Park<sup>\*a</sup>

Received 00th January 2012,  
Accepted 00th January 2012

DOI: 10.1039/x0xx00000x

www.rsc.org/

In this study, *in situ* forming gelatin hydrogels *via* horseradish peroxidase (HRP)-catalyzed cross-linking were developed to serve as bioactive wound dressings with suitable tissue adhesive properties to deliver dermal fibroblasts (DFBs). The DFBs-encapsulated gelatin hydrogels with different stiffness, GH-soft (1.1 kPa) and GH-hard (6.2 kPa), were prepared by controlling the hydrogen peroxide (H<sub>2</sub>O<sub>2</sub>) concentrations. The GH-soft hydrogel was capable of facilitating the proliferation of DFBs and the synthesis of extracellular components, as compared to GH-hard hydrogels. In addition, the subcutaneously injected GH-soft hydrogel with bioluminescent reporter cells provided enhanced cell survival and local retention over 14 days. *In vivo* transplantation of DFBs-encapsulated GH-soft hydrogels accelerated wound contraction, and promoted collagen deposition and neovascularization within the incisions performed on mice skin. Therefore, we expect that HRP-catalyzed *in situ* forming gelatin hydrogels can be useful for local delivery of cells with high viability in wounds, which holds great promise for advancing wound healing technologies and other tissue engineering applications.

### Introduction

Wound healing is a complex and interactive process in which various cellular and matrix components act together to reconstruct injured tissue.<sup>1</sup> This process comprises several overlapping phases including inflammation, proliferation and tissue remodeling. During wound healing, fibroblasts and keratinocytes in the epidermis and dermis layers of skin play a prominent role in remodeling of impaired tissue.<sup>2, 3</sup> In particular, fibroblasts primarily contribute to fill a wound bed by producing collagen and fibronectin to form new extracellular matrix (ECM). They are also known to stimulate wound contraction in the keratinocytes-enriched epidermis layer and to induce angiogenesis.<sup>4, 5</sup> However, direct cell transplantation has been shown to be inefficient in reconstructing injured tissue due to significant cell loss and the difficulty in achieving engraftment to the surrounding tissue.<sup>6</sup> To overcome these limitations, scaffold-based tissue engineering approaches have emerged and been explored over several decades.<sup>3, 7, 8</sup>

*In situ* forming hydrogels have been extensively used as promising wound dressing materials for soft tissue reconstruction.<sup>9-11</sup> They can fill irregular wound defects, absorb exudates, and retain an optimal moisture to provide an environment that supports wound healing.<sup>12</sup> For injectable cell delivery, cells can be homogeneously encapsulated inside gel matrices by simply mixing them with hydrogel precursor solutions prior to cross-linking. In addition, the encapsulated cells can survive and proliferate effectively in three-dimensional (3D) hydrogels allowing exchange of nutrients and

oxygen. Among several *in situ* gelling systems, enzymatically cross-linked hydrogels *via* a horseradish peroxidase (HRP)-catalyzed cross-linking have received considerable attention as an emerging injectable platform.<sup>13, 14</sup> This system facilitates easy manipulation of the cross-linking reaction under mild conditions, thereby achieving desirable hydrogel properties such as gelation time, mechanical stiffness and degradation rate. Despite these versatile and injectable features of the HRP-catalyzed *in situ* gelling system, there have been relatively few studies of hydrogel-based wound treatment.<sup>10, 15</sup> Wang *et al.* reported the first case of fibroblasts-encapsulated gelatin hydrogels as a wound dressing material, but they only characterized gel stiffness-dependent cell behaviors in 2D and 3D cultures. To the best of our knowledge, *in vivo* wound healing applications using the HRP-catalyzed *in situ* gelling system that carries cells are unprecedented to date. Previously, we demonstrated that the gelatin-hydroxyphenylpropionic acid (GH) hydrogel formed *via* HRP-catalyzed cross-linking exhibited highly tunable properties with good biocompatibility.<sup>16</sup> In addition, it showed strong tissue adhesion due to enzymatic cross-linking between the phenol groups of gelatin and the tyrosine residues of the tissue. These results suggest that the tissue adhesive, tunable and biocompatible GH hydrogel has potential to serve as an injectable cell delivery platform for enhanced wound healing.

We herein present DFBs-encapsulated tissue adhesive GH hydrogels as a potential gel-type wound dressing (Fig. 1). GH hydrogels were prepared using the HRP-catalyzed reaction to

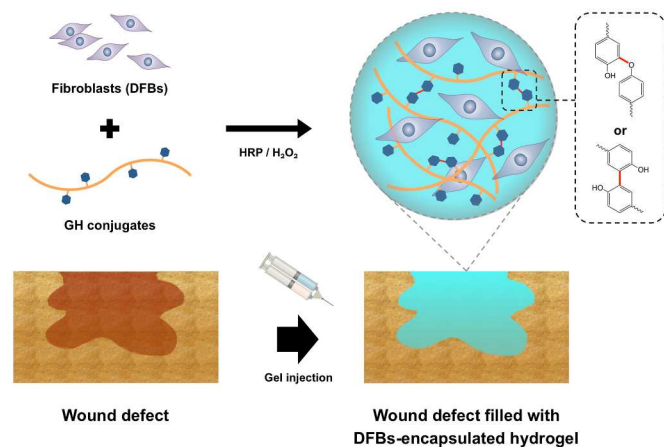


**Fig. 1** Schematic illustration of wound treatment using DFBS-encapsulated GH hydrogels formed via HRP-catalyzed cross-linking.

have different ranges of stiffness, and their properties, including elastic modulus and water-uptake ability, were characterized. The effects of hydrogel stiffness on cellular proliferative capacities (*i.e.* cell proliferation rate and changes in the production of collagen and fibronectin) were investigated by *in vitro* 3D culture. The survival and localization of DFBS encapsulated in GH hydrogels after subcutaneous injection were monitored using a bioluminescence assay. *In vivo* wound healing efficacy of DFBS-encapsulated GH hydrogels was assessed in the incisions of mice skin.

## Experimental

### Materials

Gelatin-hydroxyphenylpropionic acid (GH) conjugates were synthesized as previously described.<sup>16</sup> The phenolic content of GH was measured using a UV-vis spectrophotometer (V-750 UV/vis/NIR, Jasco, Japan) and determined to be 146.6  $\mu\text{mol}/1\text{ g}$  of GH. Peroxidase from horseradish (HRP, type VI, 250–330 units/mg solid), hydrogen peroxide ( $\text{H}_2\text{O}_2$ , 30 wt% in  $\text{H}_2\text{O}$ ), and collagenase (type II, 0.5–5.0 units/mg solid) were purchased from Sigma Aldrich (St. Louis, MO, USA). Human dermal fibroblasts (DFBS) were supplied from Lonza Inc. (Walkersville, MD, USA). Dulbecco's modified Eagle medium (DMEM), fetal bovine serum (FBS), penicillin–streptomycin (P/S), trypsin–EDTA, and Dulbecco's phosphate buffered saline (DPBS) were purchased from Gibco BRL (Grand Island, NY, USA). Live/Dead Viability/Cytotoxicity kit, Quant-iT PicoGreen dsDNA assay kit, TRIzol Reagent, and Power SYBR Green PCR master mix were purchased from Invitrogen Life Technologies (Carlsbad, CA, USA). All primers for the polymerase chain reaction (PCR) were provided from Cosmo Genetech (Seoul, Korea).

### Mechanical properties of hydrogels

The elastic modulus ( $G'$ ) of GH hydrogels was measured using a rheometer (Advanced Rheometer GEM-150-050, Bohlin Instruments, USA) in oscillation mode with a frequency of 0.1 Hz and a strain of 0.01 % using a parallel plate geometry (diameter = 25 mm, gap = 0.5 mm). 300  $\mu\text{L}$  of GH hydrogels (5 wt%) were prepared on the plate by mixing with HRP (0.002

mg/mL) and  $\text{H}_2\text{O}_2$  (0.007 or 0.02 wt%), and the elastic modulus of hydrogels was measured after 10 min at 37  $^\circ\text{C}$ .

### Morphology and water uptake behavior of hydrogels

The structure of the dried GH hydrogels was analyzed using a scanning electron microscopy (SEM; JSM-6380, JEOL, Japan). Two kinds of hydrogels with different stiffness (GH-soft and GH-hard) were prepared in a Teflon mold ( $10 \times 10 \times 50\text{ mm}^3$ ) by mixing each 200  $\mu\text{L}$  of 5% GH containing HRP (0.005 mg/mL) and  $\text{H}_2\text{O}_2$  (0.007 or 0.02 wt%). The formed hydrogels were quenched into liquid nitrogen, cross-sectioned and freeze-dried for 3 days. The morphology of dehydrated hydrogels was observed using the SEM after gold sputter coating.

To measure the water uptake ability of the GH hydrogels, the dehydrated hydrogels prepared as described above were incubated in 5 mL of PBS (0.01 M, pH 7.4) at 37  $^\circ\text{C}$  for 3 days. The weight of the swollen hydrogels ( $W_s$ ) was measured, and the degree of water uptake of hydrogels was then determined using the following equation:

$$\text{Water uptake of hydrogels (\%)} = (W_s / W_d) \times 100$$

where  $W_s$  and  $W_d$  are the weights of the swollen hydrogels and the initial dehydrated hydrogels, respectively.

### *In vitro* proteolytic degradation

The degradation rate of GH hydrogels with different cross-linking density was assessed using collagenase treatment. The total 300  $\mu\text{L}$  of GH-soft and GH-hard hydrogels were formed in microtubes. After equilibrium for 3 days, samples were incubated at 37  $^\circ\text{C}$  in 1 mL of PBS with or without 0.01 mg/mL of collagenase. At predetermined time intervals, the media were removed from microtubes and the weight of degraded hydrogels was measured. Fresh media were added then added into the tubes after weighing. The weight of the remaining hydrogels was calculated according to the following equation:

$$\text{Weight of hydrogels (\%)} = (W_d / W_i) \times 100$$

where  $W_i$  is the weight of the initial hydrogels and  $W_d$  is the weight of the degraded hydrogels.

### *In vitro* 3D culture of DFBS

*In vitro* 3D culture of DFBS was carried out to investigate stiffness-dependent cell proliferation. The GH, HRP and  $\text{H}_2\text{O}_2$  solutions were filtered using a syringe filter with a pore size of 0.2  $\mu\text{m}$  for sterilization. For the 3D cultures of DFBS encapsulated in GH hydrogels, a total 300  $\mu\text{L}$  of hydrogel was prepared in a 24-well plate as follows: (1) cells were suspended in the GH plus HRP (0.005 mg/mL) solution at a density of  $4 \times 10^5$  cells/mL; (2) the cell suspension was then mixed with the GH plus  $\text{H}_2\text{O}_2$  (0.007 or 0.02 wt%) solution. Subsequently, DMEM supplemented with 10 % FBS and 1 % P/S was added, and the media was replaced every 1–2 days over 14 days.

The number of cells that proliferated in hydrogels on 3, 7, and 14 days was determined using a PicoGreen DNA quantification assay. The cultured cells were recovered by selective degradation of hydrogels using 2.5–25 units/mL of collagenase treatment at 37  $^\circ\text{C}$  for 30 min. The solutions were centrifuged at 12,000 rpm for 5 min to obtain cell pellets. The cells were lysed with 200  $\mu\text{L}$  of RIPA lysis buffer (150 mM Trizma-base, 150 nM NaCl, 1 % sodium deoxycholate, 1 %

Triton X-100, and 0.1 % SDS in deionized water), and the solutions were mixed with 200  $\mu\text{L}$  of PicoGreen working solution. The fluorescence of the samples was measured at an excitation wavelength of 480 nm and an emission wavelength of 520 nm. The proliferation rate over 14 days was expressed as fold increase in DNA contents over control.

The morphology and viability of DFBs cultured in hydrogels were observed by optical (in phase contrast mode) and fluorescence microscope (TE-2000, Nikon, Japan). The cell viability after 14 days was assessed using a Live/Dead Viability/Cytotoxicity Assay Kit. Briefly, the cells were incubated with a mixture including 2 mM calcein AM and 4 mM ethidium homodimer-1 at 37  $^{\circ}\text{C}$  for 30 min, and then they were imaged using a fluorescence microscope.

### Reverse transcription-polymerase chain reaction (RT-PCR) analysis

The relative gene expression levels (Col I, Col III, and FN) of DFBs cultured in hydrogels were investigated by RT-PCR analysis. DFBs were encapsulated in the hydrogels at a density of  $6 \times 10^5$  cells/mL and incubated under standard cell culture conditions (37  $^{\circ}\text{C}$  and 5%  $\text{CO}_2$ ). At day 10, the encapsulated cells were harvested using the collagenase treatment as described procedure in DNA quantification assay. Total RNA was extracted from the DFBs pellet using TRIzol reagent, and processed for cDNA synthesis using a Superscript first-strand synthesis system (Invitrogen, USA). The cDNA was amplified with 30–35 cycles of PCR using gene-specific primers, as provided in Table 1. Real-time PCR was performed with the Power SYBR Green PCR master mix using a Bioneer Exicycler 96 (Bioneer Corporation, Korea). The results were normalized to GAPDH (housekeeping gene) as a reference gene, and relative gene expression levels were expressed as a fold change to the DFBs cultured on the tissue culture plate (control). All reactions were performed in triplicate.

**Table 1** Sequences of PCR primers

| Target gene | Primer sequence  |
|-------------|--|
| GAPDH       | Forward: ATGACTCCAACACGCGCAAA<br>Reverse: ATGATGACCCCTTTGGCTCC |
| Col I       | Forward: CCAGAAGAACTGGTACATCA<br>Reverse: CCGCCATACTCGAACTGGAA |
| Col III     | Forward: AGGGGAGCTGGCTACTTCTC<br>Reverse: CGGATCTGAGTCACAGACA  |
| FN          | Forward: ATGATGAGGTGCACGTGTGT<br>Reverse: CTCTTCATGACGCTTGTGGA |

GAPDH, glyceraldehyde 3-phosphatedehydrogenase; Col I, collagen type I; Col III, collagen type III; FN, fibronectin.

### In vivo monitoring of transplanted cells

Survival of cells encapsulated in the hydrogels was examined in nude mice using a bioluminescence assay. Luciferase gene-transfected cells (effluc-cells,  $1 \times 10^7$  cells/mL) kindly provided by Dr. Park (Seoul National University, Korea) were suspended in 200  $\mu\text{L}$  of GH solutions, followed by subcutaneous injection into the thighs of nude mice using a dual syringe kit where HRP

(0.02 mg/mL) and  $\text{H}_2\text{O}_2$  (0.007 or 0.02 wt%) solutions were loaded separately. Cells suspended in PBS and GH solutions were also used as controls. By 2 weeks after implantation, the bioluminescence images were acquired using IVIS-100 imaging system (Caliper Lifescience, MA, USA) after 30 min of D-luciferin treatment (150 mg/kg).

### In vivo wound healing study

Wound healing efficacy of DFBs-encapsulated GH hydrogels was evaluated with ICR mouse (male, 6 weeks of age; Orient Bio Inc., Korea). The mice were anesthetized with a Zoletil–Rompun mixture (30 mg/kg and 10 mg/kg, respectively) and then their dorsal hair was shaved and cleaned with 70 % ethanol. A full-thickness wound (10 mm in diameter) was created on the dorsal surface of each mouse, and each wound was circumscribed by donut-shaped silicone rubbers held in place using sutures to prevent wound contraction. The incisions were filled with PBS (control), GH hydrogels, and DFBs plus GH hydrogels. GH hydrogels (200  $\mu\text{L}/\text{site}$ ) containing  $7 \times 10^6$  cells/mL of DFBs were placed on the exposed wound site using a dual syringe kit in the presence of HRP (0.02 mg/mL) and  $\text{H}_2\text{O}_2$  (0.007 wt%). The filled incisions were subsequently covered with Vaseline gauze (Covidien, USA) and Neo dressing (Everaid, Korea) to minimize dehydration of hydrogels. On day 0, 4, 7, and 14 after wound treatment, a degree of re-epithelialization of tissues was evaluated by quantitatively measuring the wound area using ImageJ software (NIH, USA). The wound closure rate was determined as follows:

$$\text{Wound closure rate (\%)} = (A_0 - A_t) / A_0 \times 100$$

where  $A_0$  is the initial wound area on day 0 of the surgery and  $A_t$  is the wound area at the designated time. After 14 days of treatment, the skin was excised for histological evaluation of the healed tissue. The full thickness of skin was removed and fixed with a 10 % formalin solution. After dehydration of the fixed tissue, the samples were embedded in a paraffin block to prepare tissue sections. Masson's trichrome staining and hematoxylin and eosin (H&E) staining were performed to visualize collagen deposition and vessel formation in tissues, respectively. The animal experiments were carried out in accordance with the guidelines of Department of Laboratory Animal Resources, Yonsei University College of Medicine, Seoul, Republic of Korea.

### Statistical analysis

All data are expressed as mean  $\pm$  standard deviation. The statistical significance of the results was determined by conducting a Student's t-test.

## Results and discussion

### Characterization of GH hydrogels

The HRP-catalyzed cross-linking reaction is known to facilitate easy manipulation of mechanical stiffness of the hydrogels that appears to affect cellular responses.<sup>17, 18</sup> To investigate the effects of hydrogel stiffness on wound healing efficacy *in vitro* and *in vivo*, we first prepared two types of GH hydrogels having different mechanical stiffness. As given in Table 2, the hydrogels with distinct levels of mechanical stiffness, GH-soft



( $1.1 \pm 0.1$  kPa) and GH-hard ( $6.2 \pm 0.6$  kPa), were prepared by increasing the concentrations of  $\text{H}_2\text{O}_2$  from 0.007 to 0.02 wt%, while maintaining both polymer and HRP concentrations. Increasing the  $\text{H}_2\text{O}_2$  concentrations could lead to a greater elastic modulus due to the increased cross-linking density of hydrogel networks.<sup>16</sup> However, the highest stiffness of GH hydrogels was limited to less than 8 kPa because highly stiff hydrogels (e.g. over 10 kPa) were found to be less advantageous for a 3D cell culture system that requires sufficient transport of nutrients and matrix degradability.<sup>18</sup>

**Table 2** Preparation of GH hydrogels with different mechanical stiffness

| Sample  | Polymer (wt%) | HRP (mg/mL) | $\text{H}_2\text{O}_2$ (wt%) | $G'$ (kPa)    |
|---------|---------------|-------------|------------------------------|---------------|
| GH-soft | 5             | 0.002       | 0.007                        | $1.1 \pm 0.1$ |
| GH-hard | 5             | 0.002       | 0.020                        | $6.2 \pm 0.6$ |

Next, the effect of cross-linking density on water absorption capability of hydrogels was assessed. As shown in Fig. 2a, the equilibrium water uptake of GH-soft hydrogel was approximately 1940 % after 3 days incubation at 37 °C, which was almost two-fold higher than that of GH-hard hydrogel (1020 %). A reduced degree of cross-linking makes the structure of GH-soft hydrogel loose, thus its larger network mesh size allows absorbing a substantial amount of water. This

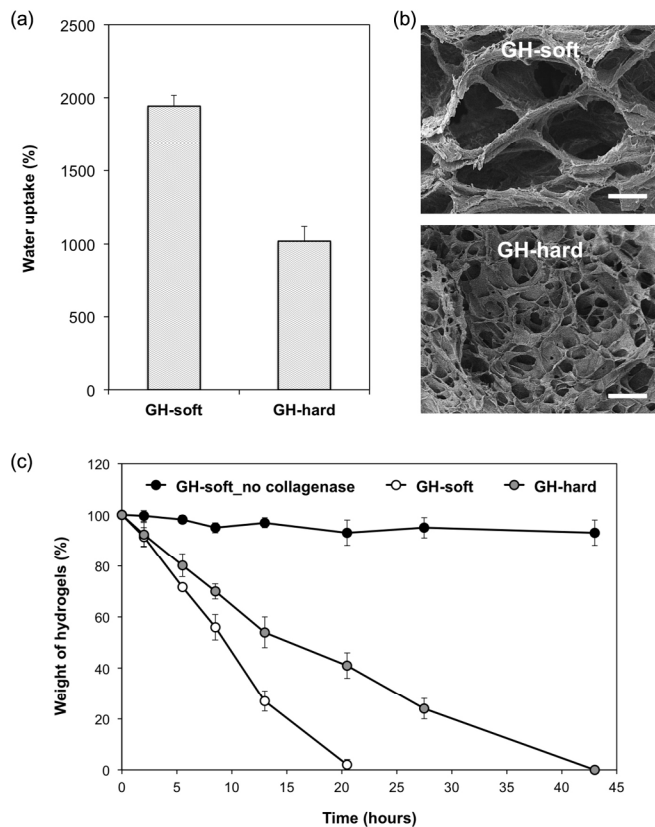


**Fig. 2** Water absorption capacity of 5 wt% GH-soft and GH-hard hydrogels ( $n=3$ ) (a) and SEM cross-sectional images of the dehydrated hydrogels (b). Scale bars represent 30  $\mu\text{m}$ . *In vitro* proteolytic degradation of GH-soft and GH-hard hydrogels ( $n=4$ ) (c).

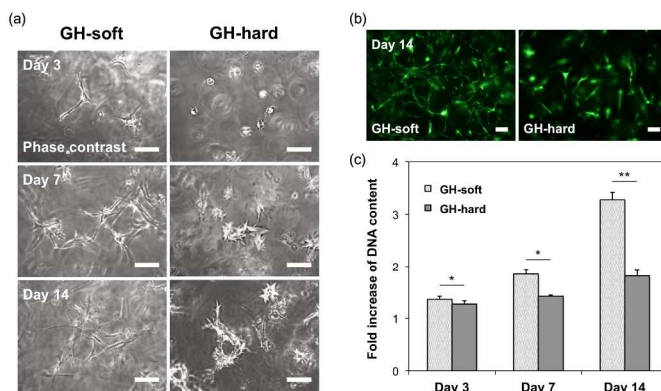


**Fig. 3** Images of the cultured DFBs in GH hydrogels with two-different stiffness for 14 days: optical (a) and live/dead staining (b) images. Cell proliferation rate of DFBs, \* $P < 0.005$  and \*\* $P < 0.001$  ( $n=3$ ) (c). Scale bars indicate 100  $\mu\text{m}$ .

inverse relationship between the mechanical stiffness and the water uptake of hydrogels can be found elsewhere.<sup>19</sup> SEM analysis was also performed to observe the porous morphology of hydrogels. The GH-soft and GH-hard hydrogels were prepared through the freeze-drying process with instantaneous quenching to minimize the influence of the dehydration process on the pore size and inner structure of hydrogels. As shown in Fig. 2b, the GH-hard hydrogel with a higher cross-linking density had smaller pores than those observed in the cross-section of the GH-soft hydrogel.

We also investigated *in vitro* proteolytic degradation rates of GH hydrogels with different stiffness in the presence of collagenase. The GH-soft and GH-hard hydrogels were completely degraded within 21 h and 43 h, respectively, whereas the GH-soft hydrogel incubated in PBS without treating collagenase were constantly stable. This result indicates that the degradation rate of GH hydrogels is dependent on their cross-linking density (Fig. 2c).

### Effects of hydrogel stiffness on cellular activities

Cellular behavior such as spreading, viability, and proliferation was evaluated by culturing DFBs encapsulated in GH hydrogels with different stiffness (1.1 and 6.2 kPa) for 14 days. As shown in Fig. 3a, the DFBs in GH-soft hydrogels revealed excellent spreading as compared to those in GH-hard hydrogels. On day 3, most of the encapsulated cells readily showed spindle-like and well-elongated morphologies in GH-soft hydrogels. In addition, interconnected networks with surrounding cells were formed by day 14, indicating that a hydrogel with low stiffness is advantageous for cell spreading and cell-cell interactions. On the contrary, cells cultured in GH-hard hydrogels appeared to have difficulty spreading. Therefore, the cells in GH-soft hydrogels could show more spreading morphology due to the relatively faster degradation rate of gelatin matrix as both spreading and migration of encapsulated cells can only occur with the digestion of cross-linked polymers.<sup>20</sup>

As for cell viability, the majority of the cells in all hydrogels were viable (stained green) even after 14 days of culture, and no dead cells were detected (stained red) (Fig. 3b). The density of cells proliferating in hydrogels was quantitatively measured by comparing initial DNA content of seeded cells on day 0 with those on day 3, 7, and 14 (Fig. 3c). The encapsulated hDFBs were found to be more proliferative

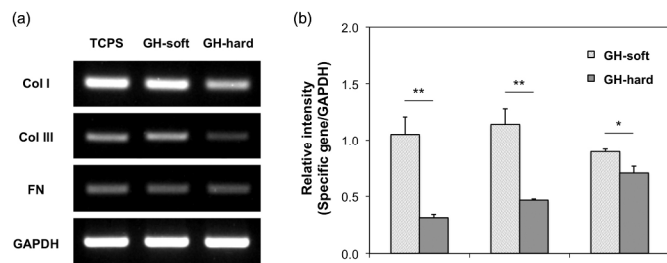


**Fig. 4** mRNA expression levels of Col I, Col III, FN, and GAPDH expressed from DFBs on day 10 (a) and normalized expression profiles with respect to the GAPDH expression based on TCPS as the control group, \* $P < 0.05$  and \*\* $P < 0.005$  ( $n = 3$ ) (b).

when the hydrogel was less stiff, which is in good agreement with previously reported data.<sup>15, 21</sup> It was demonstrated that further increases of cross-linking density in hydrogels resulted in decreased permeability and thus led to the limited cellular activities in the 3D cell culture environment.

### Gene expression of DFBs in gelatin hydrogels

As ECM components are required for the wound healing process, the gene expression levels of FN, Col I, and Col III from DFBs cultured in GH hydrogels were analyzed by the real time RT-PCR (Fig. 4). For comparison, the same number of cells was cultured on a cell culture plate (TCPS) without hydrogels. Col I and Col III in the cells in GH-hard hydrogels were down-regulated as compared to TCPS. In the case of GH-soft hydrogels, however, no significant differences were found in the expression profiles of FN, Col I and Col III. Additionally, DFBs showed 1.3–3.7 times higher levels of gene expression when the hydrogel stiffness was decreased from 6.2 to 1.1 kPa. A similar trend was reported by Ayala *et al.*, demonstrating that the hydrogel stiffness modulates the level of mRNA expression from DFBs and thereby promotes the ECM synthesis.<sup>22</sup> Given together that the GH-soft hydrogel enables a better proliferation of DFBs and ECM synthesis than the GH-hard hydrogel, these results suggest that the GH-soft hydrogel serves as a more suitable vehicle for cell delivery.

### *In vivo* monitoring of cells encapsulated in hydrogels

To investigate *in vivo* survival of cells transplanted with hydrogels, GH hydrogels containing effluc-cells were injected subcutaneously into the thigh of nude mice and monitored over 14 days. As controls, cells suspended in PBS or non-crosslinked GH solutions were also injected (Fig. 5a and b). After D-luciferin administration, the luciferase signals were observed through a catalytic reaction of luciferase. As shown in Fig. 5c and d, both GH-soft and GH-hard hydrogels had very weak fluorescence intensities when compared to control groups (Fig. 5a and b), which might be due to time-dependent penetration of D-luciferin into gel matrix for the reaction. However, their intensities became strong at day 2 and then gradually decreased, indicating that GH hydrogels were associated with a prolonged survival of encapsulated effluc-cells by minimizing cell loss and facilitating cell expansion. Furthermore, effluc-cells in GH-soft hydrogels exhibited higher cell proliferation than those in GH-hard hydrogels. These results clearly demonstrate that matrix stiffness plays a vital role for cell growth both *in vitro* and *in vivo*.<sup>23</sup> On the contrary,

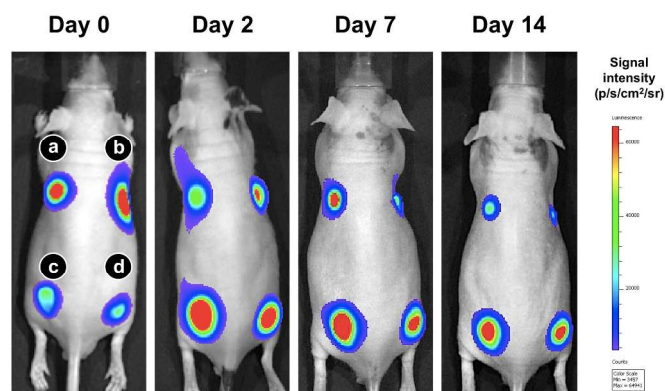


**Fig. 5** Bioluminescence images of effluc-cells incorporated in PBS (a), non-crosslinked GHPA solutions (b), GH-soft hydrogels (c), and GH-hard hydrogels (d) at different time points (on day 0, 2, 7, 14).

the cells in non-crosslinked solution showed low levels of retention and survival at the point of injection area.

### *In vivo* wound healing and histological examination

To assess *in vivo* wound-healing efficacy of DFBs plus GH hydrogels, full-thickness skin incisions were created on the back of mice, and then prepared samples were applied on the top of wound sites. In this experiment, we choose the GH-soft hydrogel that previously appeared more suitable for enhanced cell proliferation and collagen production in the 3D culture environments. Fig. 6a shows images of skin wounds taken at different time intervals after treating with PBS, GH hydrogels and DFBs plus GH hydrogels, respectively. It is clearly observed that in all treated wound lesions, the growth of new epidermis was extended to the wound centers, thus resulting in the reduced area of wounds. Among the treatment groups, DFBs plus GH hydrogels revealed the most accelerated wound contraction up to 14 days, as compared with PBS and GH-soft hydrogels only (Fig. 6b). Particularly, the treatment of DFBs plus GH hydrogels led to improved early healing of the wounds. At 4 days post-transplantation, the wound closure rate of DFBs plus GH hydrogels reached about 33%, whereas PBS and GH hydrogels alone had lower wound closure rates (17% and 18%, respectively). This result might be due to enhanced proliferation of keratinocytes and re-epithelialization by transplanted DFBs.<sup>5, 24</sup> It is also reported that fibroblasts contribute to generating the contractile force at the wound area, where this process mostly occurs at the initial stage of wound healing.<sup>8</sup>

Collagen is a predominant structural protein in skin, which is necessary to effectively reconstruct the dermis tissue at wound sites.<sup>7</sup> After 14 days of treatment, retrieved tissues were processed for Masson's trichrome staining to identify collagen. A more intense blue color was observed in the wound tissue covered with DFBs plus GH hydrogels (Fig. 6c), indicating that collagen deposition by DFBs proliferated in the GH hydrogel was more mature than other samples. Moreover, the H&E staining confirmed the formation of new microvessels in the reconstructed dermis tissue. Particularly, a considerable increase in vascularization was observed in the group treated with DFBs plus GH hydrogels. It is known that DFBs produce potent angiogenic factors such as basic fibroblast growth factor (bFGF) and interleukin-8 (IL-8) that can contribute to angiogenic effects.<sup>25</sup> In addition, several previous studies



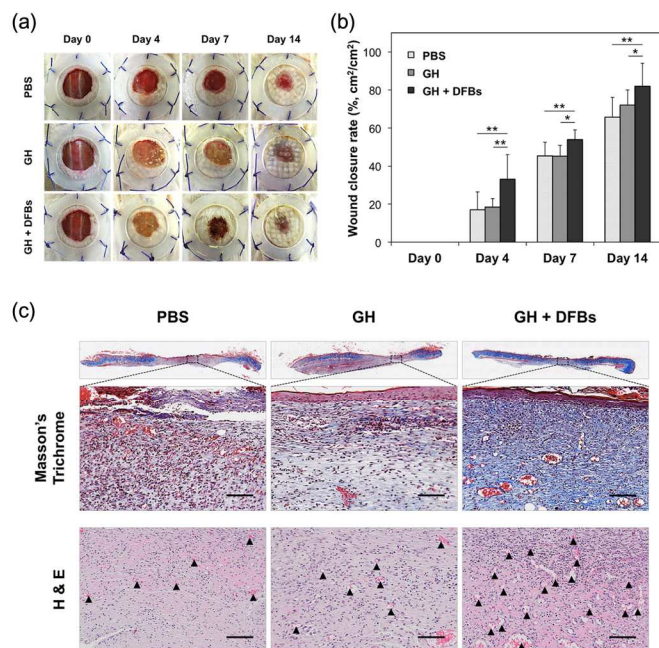


**Fig. 6** Photographs (a) and closure rate (b) of wounds treated with PBS (control), GH hydrogels, and DFBs plus GH hydrogels during the wound healing process for 14 days, \* $P < 0.1$  and \*\* $P < 0.05$  ( $n = 3$ ). Representative images of Masson's Trichrome and H&E stained histological sections on 14 days after transplantation (c). Arrows (▲) indicate microvessels. Scale bars indicate 100  $\mu\text{m}$ .

demonstrated that DFBs dominantly support and modulate endothelial cells migration, viability, and vessel network formation in a co-culture system with DFBs.<sup>26, 27</sup> These data also support that the DFBs encapsulated in the GH-soft hydrogel could promote neovascularization during wound healing.

## Conclusions

The present study demonstrates injectable gelatin hydrogels as a tissue adhesive wound dressing material to deliver fibroblasts for wound healing applications. The gelatin hydrogels were formed *via* HRP-catalyzed reaction, and matrix stiffness-dependent cellular responses were investigated by encapsulating DFBs in GH hydrogels with different elastic moduli. The softer hydrogel showed relatively superior potential in cell proliferation rate and the production of ECM components (Col I, Col III and FN). Moreover, *in vivo* monitoring of subcutaneously injected cells revealed that the hydrogels facilitated cell survival and retention at the point of injection site. Finally, we demonstrated that the incorporation of DFBs into GH hydrogels led to the accelerated wound contraction, the promoted the mature collagen deposition and neovascularization in the incision sites of mice skin. Therefore, we expect that HRP-catalyzed *in situ* cross-linkable GH hydrogels can serve as a promising cell delivery platform not only for wound healing but also for other tissue engineering applications.

## Acknowledgements

This work was supported by Basic Science Research Program through the National Research Foundation of Korea (NRF) grant funded by the Ministry of Science, ICT & Future Planning (NRF-2012R1A2A2A06046885), and the Ministry of Education (2009-0093826).

## Notes and references

<sup>a</sup> Department of Molecular Science and Technology, Ajou University, Suwon 443-749, Republic of Korea. E-mail: kdp@ajou.ac.kr; Fax: +82-31-219-1592; Tel: +82-31-219-1846

<sup>b</sup> Department of Orthopaedic Surgery, Yonsei University College of Medicine, Seoul 120-752, Republic of Korea

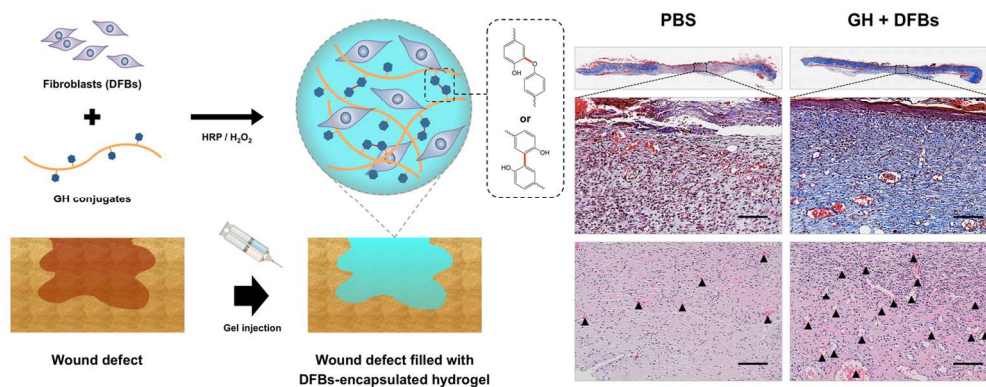
<sup>c</sup> College of Pharmacy, School of Medicine, Ajou University, Suwon 443-749, Republic of Korea

1. A. J. Singer and R. A. Clark, *N. Engl. J. Med.*, 1999, **341**, 738.
2. T. Zuliani, S. Saiagh, A. C. Knol, J. Esbelin and B. Dreno, *PLoS One*, 2013, **8**, e70408.
3. E. J. Yun, B. Yon, M. K. Joo and B. Jeong, *Biomacromolecules*, 2012, **13**, 1106.
4. D. Liu and P. J. Hornsby, *Neoplasia*, 2007, **9**, 418.
5. T. Svensjo, F. Yao, B. Pomahac, T. Winkler and E. Eriksson, *Transplantation*, 2002, **73**, 1033.
6. K. C. Rustad, V. W. Wong, M. Sorkin, J. P. Glotzbach, M. R. Major, J. Rajadas, M. T. Longaker and G. C. Gurtner, *Biomaterials*, 2012, **33**, 80.
7. W. Y. Huang, C. L. Yeh, J. H. Lin, J. S. Yang, T. H. Ko and Y. H. Lin, *J. Mater. Sci. Mater. Med.*, 2012, **23**, 1465.
8. P. Y. Lee, E. Cobain, J. Huard and L. Huang, *Mol. Ther.*, 2007, **15**, 1189.
9. S. S. Anumolu, A. R. Menjoge, M. Deshmukh, D. Gerecke, S. Stein, J. Laskin and P. J. Sinko, *Biomaterials*, 2011, **32**, 1204.
10. N. Q. Tran, Y. K. Joung, E. Lih and K. D. Park, *Biomacromolecules*, 2011, **12**, 2872.
11. B. Kundu and S. C. Kundu, *Biomaterials*, 2012, **33**, 7456.
12. Z. Fan, B. Liu, J. Wang, S. Zhang, Q. Lin, P. Gong, L. Ma and S. Yang, *Adv. Funct. Mater.*, 2014, **24**, 3933.
13. L. S. Teixeira, J. Feijen, C. A. van Blitterswijk, P. J. Dijkstra and M. Karperien, *Biomaterials*, 2012, **33**, 1281.
14. K. H. Bae, L. S. Wang and M. Kurisawa, *J. Mater. Chem. B*, 2013, **1**, 5371.
15. L. S. Wang, J. E. Chung and M. Kurisawa, *J. Biomater. Sci., Polym. Ed.*, 2011, **23**, 1793.
16. Y. Lee, J. W. Bae, D. H. Oh, K. M. Park, Y. W. Chun, H. J. Sung and K. D. Park, *J. Mater. Chem. B*, 2013, **1**, 2407.
17. L. S. Wang, C. Du, W. S. Toh, A. C. Wan, S. J. Gao and M. Kurisawa, *Biomaterials*, 2014, **35**, 2207.
18. K. M. Park, K. S. Ko, Y. K. Joung, H. Shin and K. D. Park, *J. Mater. Chem.*, 2011, **21**, 13180.
19. R. Devolder, E. Antoniadou and H. Kong, *J. Controlled Release*, 2013, **172**, 30-37.
20. P. B. Welzel, M. Grimmer, C. Renneberg, L. Naujox, S. Zschoche, U. Freudenberg and C. Werner, *Biomacromolecules*, 2012, **13**, 2349.

## Journal Name

21. J. W. Nichol, S. T. Koshy, H. Bae, C. M. Hwang, S. Yamanlar and A. Khademhosseini, *Biomaterials*, 2010, **31**, 5536.
22. P. Ayala, J. I. Lopez and T. A. Desai, *Tissue Eng., Part A*, 2010, **16**, 2519.
23. A. Lathuiliere, S. Cosson, M. P. Lutolf, B. L. Schneider and P. Aebischer, *Biomaterials*, 2014, **35**, 779.
24. P. Velander, C. Theopold, O. Bleiziffer, J. Bergmann, H. Svensson, Y. Feng and E. Eriksson, *J. Surg. Res.*, 2009, **157**, 14.
25. T. A. Martin, K. G. Harding and W. G. Jiang, *Angiogenesis*, 1999, **3**, 69.
26. A. C. Newman, M. N. Nakatsu, W. Chou, P. D. Gershon and C. C. Hughes, *Mol. Biol. Cell*, 2011, **22**, 3791.
27. L. A. Kunz-Schughart, J. A. Schroeder, M. Wondrak, F. van Rey, K. Lehle, F. Hofstaedter and D. N. Wheatley, *Am. J. Physiol.: Cell Physiol.*, 2006, **290**, C1385.





Wound treatment using injectable or sprayable fibroblast-encapsulated GH hydrogels  
138x54mm (300 x 300 DPI)